

NUMERICAL MODELLING OF VISCOUS AND VISCOELASTIC FLUIDS FLOW

Radka Keslerová / Karel Kozel

Department of Technical Mathematics, Faculty of Mechanical Engineering, Czech Technical University, Praha

Introduction

Generalized Newtonian fluids can be subdivided according to viscosity behavior. For Newtonian fluids viscosity is constant and is independent of the applied shear stress (eg. water, kerosene etc.). Shear thinning fluids are characterized by decreasing viscosity with increasing shear rate (eg. ketchup, honey, blood etc). Shear thickening fluids are characterized by increasing viscosity with increasing shear rate (eg. wet sand etc.). In the case that for blood an elastic effect is assumed then blood is considered as the viscoelastic fluid (generalized Oldroyd-B fluids).

Mathematical Model

The governing system of equations is the system of balance laws of mass and momentum for incompressible fluids [1], [3]:

$$\operatorname{div} \mathbf{u} = 0 \quad (1)$$

$$\rho \frac{\partial \mathbf{u}}{\partial t} + \rho(\mathbf{u} \cdot \nabla) \mathbf{u} = -\nabla P + \operatorname{div} \mathbf{T} \quad (2)$$

where P is pressure, ρ is constant density, \mathbf{u} is velocity vector. The symbol \mathbf{T} represents stress tensor with different definition.

a) Viscous fluids

The simple viscous model is *Newtonian model*:

$$\mathbf{T} = 2\mu \mathbf{D} \quad (3)$$

where μ is dynamic viscosity and tensor \mathbf{D} is symmetric part of velocity gradient.

b) Viscoelastic fluids

Maxwell model is the simplest model for viscoelastic fluid. In this case the stress tensor is computed from:

$$\mathbf{T} + \lambda_1 \frac{\delta \mathbf{T}}{\delta t} = 2\mu \mathbf{D} \quad (4)$$

where λ_1 has dimension of time and denotes *relaxation time*. The symbol $\frac{\delta}{\delta t}$ represents upper convected derivative (see eq. (8)).

The behavior of the mixture of viscous and viscoelastic fluids can be described by *Oldroyd-B model* and it has the form

$$\mathbf{T} + \lambda_1 \frac{\delta \mathbf{T}}{\delta t} = 2\mu \left(\mathbf{D} + \lambda_2 \frac{\delta \mathbf{D}}{\delta t} \right). \quad (5)$$

The parameters λ_1, λ_2 are *relaxation* and *retardation time*.

The stress tensor \mathbf{T} is decomposed to Newtonian part \mathbf{T}_s and viscoelastic part \mathbf{T}_e ($\mathbf{T} = \mathbf{T}_s + \mathbf{T}_e$) and

$$\mathbf{T}_s = 2\mu_s \mathbf{D}, \quad \mathbf{T}_e + \lambda_1 \frac{\delta \mathbf{T}_e}{\delta t} = 2\mu_e \mathbf{D}, \quad (6)$$

where

$$\frac{\lambda_2}{\lambda_1} = \frac{\mu_s}{\mu_s + \mu_e}, \quad \mu = \mu_s + \mu_e. \quad (7)$$

The *upper convected derivative* $\frac{\delta}{\delta t}$ is defined (for general tensor) by the relation (see [3])

$$\frac{\delta \mathbf{M}}{\delta t} = \frac{\partial \mathbf{M}}{\partial t} + (\mathbf{u} \cdot \nabla) \mathbf{M} - (\mathbf{W} \mathbf{M} - \mathbf{M} \mathbf{W}) - (\mathbf{D} \mathbf{M} + \mathbf{M} \mathbf{D}) \quad (8)$$

where \mathbf{D} is the symmetric part of the velocity gradient $\mathbf{D} = \frac{1}{2}(\nabla \mathbf{u} + \nabla \mathbf{u}^T)$ and \mathbf{W} is the antisymmetric part of the velocity gradient $\mathbf{W} = \frac{1}{2}(\nabla \mathbf{u} - \nabla \mathbf{u}^T)$.

The governing system (1), (2) of equations is completed by the equation for the viscoelastic part of the stress tensor

$$\frac{\partial \mathbf{T}_e}{\partial t} + (\mathbf{u} \cdot \nabla) \mathbf{T}_e = \frac{2\mu_e}{\lambda_1} \mathbf{D} - \frac{1}{\lambda_1} \mathbf{T}_e + (\mathbf{W} \mathbf{T}_e - \mathbf{T}_e \mathbf{W}) + (\mathbf{D} \mathbf{T}_e + \mathbf{T}_e \mathbf{D}). \quad (9)$$

Both models could be generalized. In this case the viscosity μ is no more constant, but is defined by viscosity function according to the cross model

$$\mu(\dot{\gamma}) = \mu_\infty + \frac{\mu_0 - \mu_\infty}{(1 + (\lambda \dot{\gamma})^b)^a} \quad (10)$$

where

$$\dot{\gamma} = 2\sqrt{\frac{1}{2} \text{tr} \mathbf{D}^2} \quad (11)$$

$$\begin{aligned} \mu_0 &= 1.6 \cdot 10^{-1} Pa \cdot s & \mu_\infty &= 3.6 \cdot 10^{-3} Pa \cdot s \\ a &= 1.23, b = 0.64 & \lambda &= 8.2s. \end{aligned}$$

Numerical Solution

Numerical solution of the described models is based on cell-centered finite volume method using explicit Runge–Kutta time integration. The unsteady system of equations with steady boundary conditions is solved by finite volume method. Steady state solution is achieved for $t \rightarrow \infty$. In this case the artificial compressibility method can be applied. It means that the continuity equation is completed by the time derivative of the pressure in the form (for more details see e.g. [2]):

$$\frac{1}{\beta^2} \frac{\partial p}{\partial t} + \text{div} \mathbf{u} = 0, \quad \beta \in \mathbb{R}^+. \quad (12)$$

The system of equations (including the modified continuity equation) could be rewritten in the vector form for 2D case. For 3D case it's similar but more complicated.

$$\tilde{R}_\beta W_t + F_x^c + G_y^c = F_x^v + G_y^v + S, \quad \tilde{R}_\beta = \text{diag}\left(\frac{1}{\beta^2}, 1, 1, 1, 1, 1\right). \quad (13)$$

where W is the vector of unknowns, F^c, G^c are inviscid fluxes, F^v, G^v are viscous fluxes defined as

$$W = \begin{pmatrix} p \\ u \\ v \\ t_{11} \\ t_{12} \\ t_{22} \end{pmatrix}, \quad F^c = \begin{pmatrix} u \\ u^2 + p \\ uv \\ ut_{11} \\ ut_{12} \\ ut_{22} \end{pmatrix}, \quad G^c = \begin{pmatrix} v \\ uv \\ v^2 + p \\ vt_{11} \\ vt_{12} \\ vt_{22} \end{pmatrix}, \quad (14)$$

$$F^v = \begin{pmatrix} 0 \\ 2\mu(\dot{\gamma})u_x \\ \mu(\dot{\gamma})(u_y + v_x) \\ 0 \\ 0 \\ 0 \end{pmatrix}, \quad G^v = \begin{pmatrix} 0 \\ \mu(\dot{\gamma})(u_y + v_x) \\ 2\mu(\dot{\gamma})v_y \\ 0 \\ 0 \\ 0 \end{pmatrix} \quad (15)$$

and the source term S is defined as where t_{ij} are components of the symmetric tensor \mathbf{T}_e

$$S = \begin{pmatrix} 0 \\ t_{11x} + t_{12y} \\ t_{12x} + t_{22y} \\ 2\frac{\mu_e}{\lambda_1}u_x - \frac{t_{11}}{\lambda_1} + 2(u_x t_{11} + u_y t_{12}) \\ \frac{\mu_e}{\lambda_1}(u_y + v_x) - \frac{t_{12}}{\lambda_1} + (u_x t_{12} + u_y t_{22} + v_x t_{11} + v_y t_{12}) \\ 2\frac{\mu_e}{\lambda_1}v_y - \frac{t_{22}}{\lambda_1} + 2(v_x t_{12} + v_y t_{22}) \end{pmatrix} \quad (16)$$

The following testcases are considered for numerical computation:

Newtonian	$\mu(\dot{\gamma}) = \mu_s = const.$	$\mathbf{T}_e \equiv 0$
Generalized Newtonian	$\mu(\dot{\gamma})$	$\mathbf{T}_e \equiv 0$
Oldroyd-B	$\mu(\dot{\gamma}) = \mu_s = const.$	\mathbf{T}_e
Generalized Oldroyd-B	$\mu(\dot{\gamma})$	\mathbf{T}_e

The eq. (13) is discretized in space by the cell-centered finite volume method (see [5]) and the arising system of ODEs is integrated in time by the explicit multistage Runge–Kutta scheme (see [4], [6]):

$$\begin{aligned} W_i^n &= W_i^{(0)} \\ W_i^{(s)} &= W_i^{(0)} - \alpha_{s-1} \Delta t \mathcal{R}(W)_i^{(s-1)} \\ W_i^{n+1} &= W_i^{(M)} \quad s = 1, \dots, M, \end{aligned} \quad (17)$$

where $M = 3$, $\alpha_0 = \alpha_1 = 0.5$, $\alpha_2 = 1.0$, the steady residual $\mathcal{R}(W)_i$ is defined as

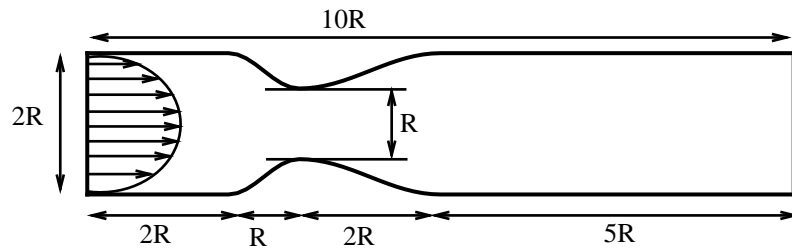
$$\mathcal{R}(W)_i = \frac{1}{\sigma_i} \sum_{k=1}^4 [(\overline{F}_k^c - \overline{F}_k^v) \Delta y_k - (\overline{G}_k^c - \overline{G}_k^v) \Delta x_k] + \overline{S}, \quad (18)$$

where σ_i is the volume of cell, $\sigma_i = \int \int_{C_i} dx dy$. The symbols $\overline{F}_k^c, \overline{G}_k^c$ and $\overline{F}_k^v, \overline{G}_k^v$ denote numerical approximation of inviscid and viscous fluxes, for more details see [4], symbol \overline{S} represents

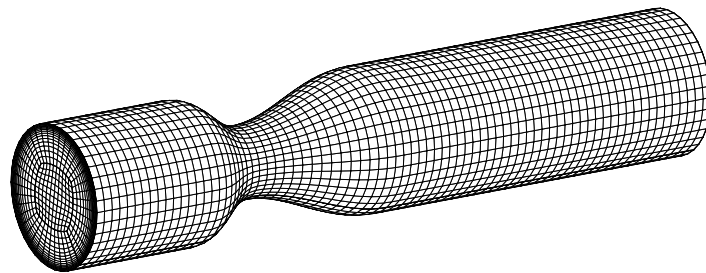
numerical approximation of the source term with central approximation of derivatives.

Numerical results

Four testcases of generalized Newtonian and Oldroyd-B fluids flow are presented and compared. In the figs. 1 and 2 the structure of tested domain is shown.



Obrázek 1: Structure of computational domain.



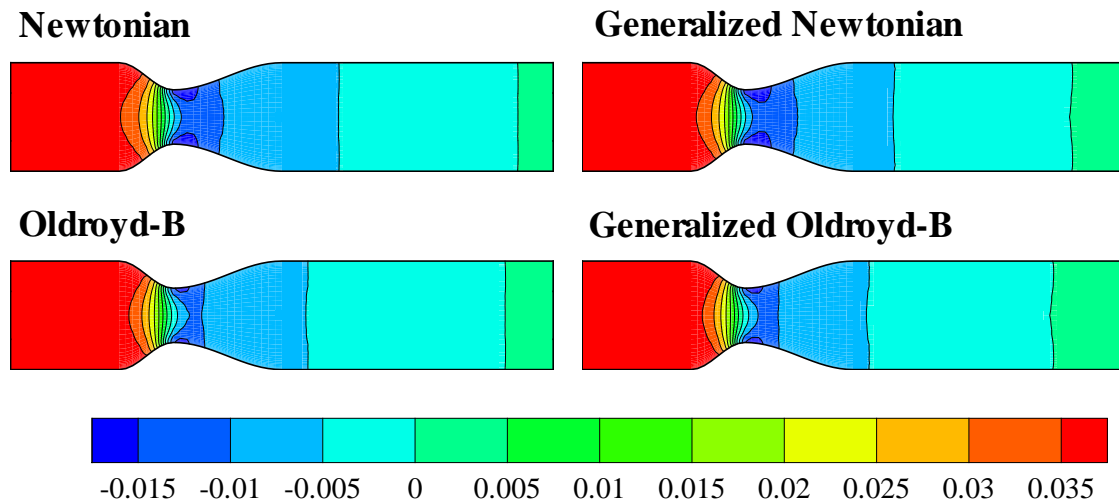
Obrázek 2: Structure of computational mesh.

The following model parameters are:

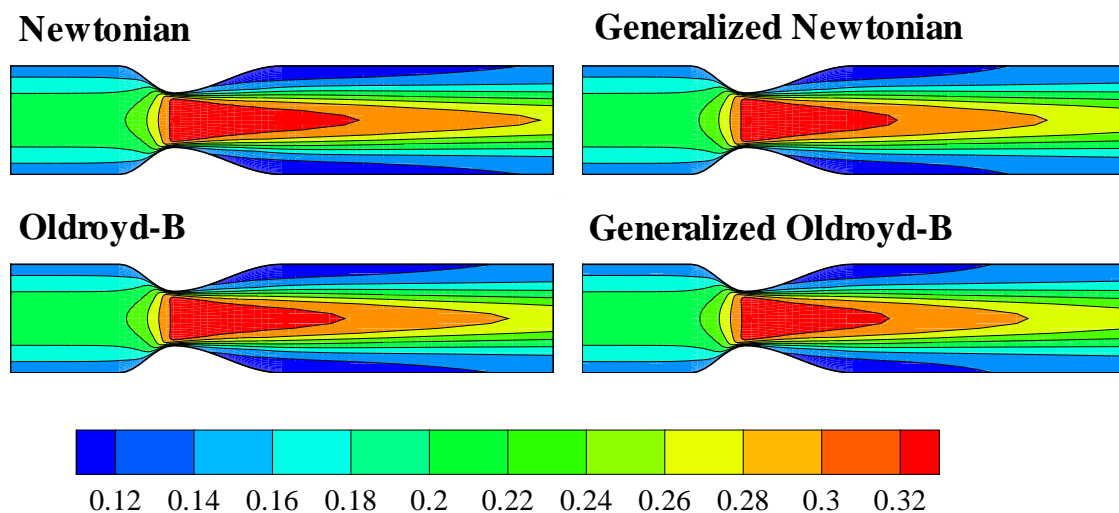
$$\begin{aligned} \mu_e &= 4.0 \cdot 10^{-4} Pa \cdot s & \mu_s &= 3.6 \cdot 10^{-3} Pa \cdot s \\ \lambda_1 &= 0.06s & \lambda_2 &= 0.054s \\ U_0 &= 0.0615m \cdot s^{-1} & L_0 &= 2R = 0.0062m \\ \mu_0 = \mu &= \mu_s + \mu_e & \rho &= 1050kg \cdot m^{-3} \end{aligned}$$

In the Figs. 3 and 4 the comparison of the axial velocity isolines and the pressure distributions is presented.

Pressure and velocity distribution along the axis for all tested fluids models is shown in the Fig. 5. By simple observation one can conclude that the main effect of the Oldroyd-B fluids behavior is visible mainly in the recirculation zone.



Obrázek 3: Pressure distribution.

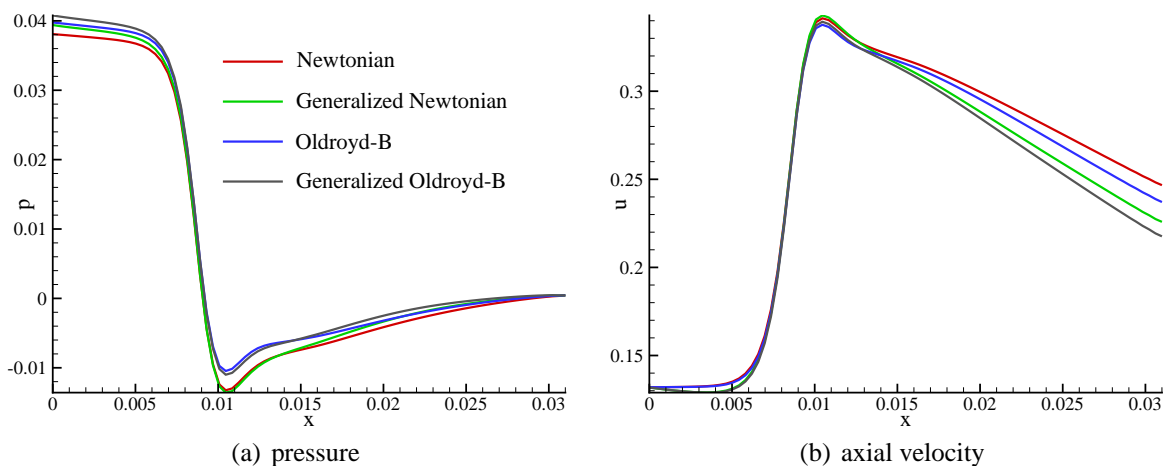


Obrázek 4: Axial velocity distribution.

Conclusions

Newtonian and Oldroyd-B models with their generalized modification have been considered for numerical simulation of fluids flow in the idealized axisymmetric stenosis. The cell-centered finite volume solver for incompressible laminar viscous and viscoelastic fluids flow has been described. In the idealized stenosis we tested the generalized Newtonian and generalized Oldroyd-B fluids models. Here the two definitions of the stress tensor were used. Based on the above numerical results we can conclude that the difference between the viscous and viscoelastic fluids is visible in the recirculation zone.

Acknowledgement: This work was partly supported by the grant GACR 101/09/1539 and



Obrázek 5: Pressure and axial velocity distribution along the central axis of the channel.

GACR 201/09/0917, Research Plan MSM 684 077 0003 and Research Plan MSM 684 077 0010.

Reference

- [1] R. Dvořák and K. Kozel: *Mathematical Modelling in Aerodynamics (in Czech)*. CTU, Prague, Czech Republic, 1996.
- [2] A.J. Chorin, A numerical method for solving incompressible viscous flow problem, *Journal of Computational Physics* **135** (1967) 118–125.
- [3] T. Bodnar and A. Sequeira, Numerical Study of the Significance of the Non-Newtonian Nature of Blood in Steady Flow through a Stenosed Vessel (Editor: R. Ranacher, A. Sequeira), *Advances in Mathematical Fluid Mechanics* (2010) 83–104.
- [4] R. Keslerová and K. Kozel, Numerical modelling of incompressible flows for Newtonian and non-Newtonian fluids, *Journal of Mathematics and Computers in Simulation* **80** (2010) 1783–1794.
- [5] R. LeVeque: *Finite-Volume Methods for Hyperbolic Problems*. Cambridge University Press, 2004.
- [6] J. Vimmr and A. Jonášová, Non-Newtonian Effects of Blood Flow in Complete Coronary and Femoral Bypasses, *Mathematics and Computers in Simulation* **80** (2010) 1324–1336.